

## TECHNICAL PAPER

Journal of the South African  
Institution of Civil Engineering, 46(4)  
2004, Pages 20–24, Paper 578



R SENTHIVEL BEng, MTech, PhD, MIE(I), MISTE obtained his master's and doctoral degrees from the National Institute of Technology, India, and Indian Institute of Technology, Delhi, respectively. He has post-doctoral research experience in masonry in the USA and Germany and is currently employed as a postdoctoral research fellow at the University of the Witwatersrand. He has written several research papers in the area of structural masonry.



H C UZOEGBO PrEng, MSc, DIC, PhD, MSAICE obtained an MEng in civil engineering from the Technical University of Bucharest. He also obtained MSc, DIC and PhD in concrete structures from the University of London. He worked for

two years in the construction industry before embarking on a university teaching career. He has since taught and carried out research in structural engineering at universities in Nigeria, Zambia, Zimbabwe and currently at the University of the Witwatersrand.

Keywords: pseudo dynamic, masonry, stress-strain curve, common points, stability points

# Failure criterion of unreinforced masonry under biaxial pseudo dynamic loading

R Senthivel and H C Uzoegbo

*Experimental tests on scaled unreinforced calcium silicate brick masonry (URM) panels subjected to pseudo dynamic biaxial compression were conducted for five principal stress ratios. Envelope curves, common point curves and stability point curves were established. The peak stresses of these curves were used to obtain a family of failure interaction curves. A general expression for the failure interaction curves is proposed in terms of principal stress invariants. The stability point failure interaction curve provides a rational design tool in defining the permissible stress levels of calcium silicate brick masonry under in-plane pseudo dynamic loading.*

## INTRODUCTION

Most masonry wall structures such as shear walls, infill panels in framed construction, beam footing, etc, are subjected to in-plane vertical and lateral loads and hence are in a state of planar biaxial stress. In-plane loads can act pseudo dynamically (eg seismic loads), thus inducing a pseudo dynamic biaxial stress state in various regions of the

masonry structural element. Depending on the location within the structural element, the biaxial stress states can be compressive-compressive, compressive-tensile or tensile-tensile. A number of research studies have reported on the behaviour of masonry under biaxial stress states. Most of the research efforts have been directed towards establishing a failure surface of the material (Samarasinghe 1980, Page 1981, 1982,

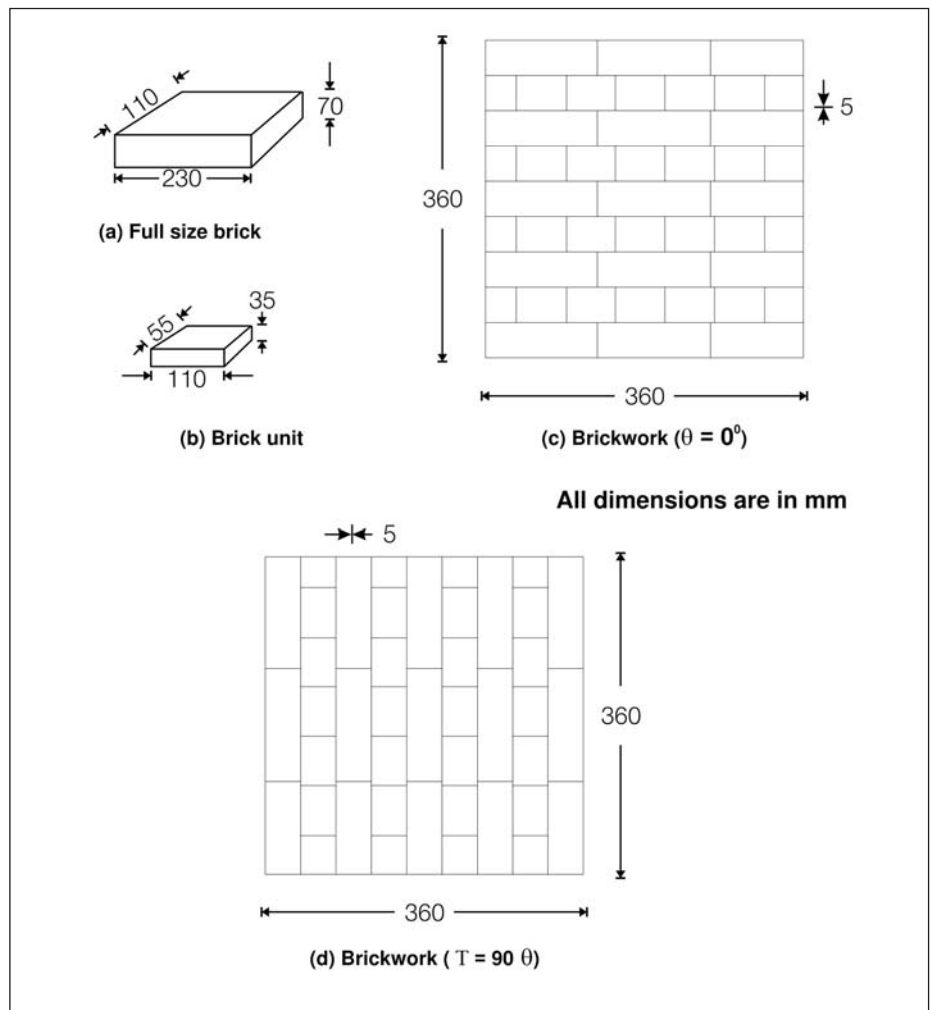


Figure 1 Details of test panels

Dhanasekar 1985). Investigations have also been conducted to study the deformation characteristics of brick masonry under biaxial stress states (Dhanasekar *et al* 1985). However, the results reported in respect of the behaviour of brick masonry under biaxial stress states are limited to tests under monotonic loading. It was only during the last decade that investigation on the behaviour of brick masonry under pseudo dynamic biaxial stress states have been attempted by Naraine and Sinha (1992). However, such studies were limited to brick masonry made with clay bricks of low strength.

This paper presents experimental investigation of the behaviour of calcium silicate brick masonry under pseudo dynamic biaxial compressive-compressive loading. The present study is an extension of the investigation on the behaviour of brick masonry under pseudo dynamic uniaxial compressive loading reported elsewhere. The experimental programme of the investigation involved biaxial tests on as many as 60 half-scale calcium silicate brick masonry specimens for the following stress ratios:

$$f = f_n/f_p = 0, 1, 2, 4 \text{ and } 10$$

Where  $f$  = stress ratio  
 $f_n$  = stress applied in vertical direction  
 $f_p$  = stress applied in horizontal direction

Three types of tests were conducted to establish the envelope stress-strain curve, the common point curve and the stability point curve of the calcium silicate brick masonry for each biaxial stress ratio. A failure criterion for modelling the limiting failure stress state expressed in terms of principal stress invariants has been proposed.

## EXPERIMENTAL PROGRAMME

The experimental programme involved testing half-scale calcium silicate brick masonry models under pseudo dynamic biaxial loading that induced compression-compression stress state. The angle of inclination between the horizontal principal stresses and the bed joints were limited to 0° and 90°.

## Test specimens

A full-scale solid calcium silicate brick unit measures 230 mm x 110 mm x 70 mm. Eight half-scale brick units measuring 115 mm x 55 mm x 35 mm were sawn out from each full brick. Based on a sample of 30 half-scale bricks, the average compressive strength was found to be 23,6 MPa. A 1:1/2:4 mix by volume of cement, lime and sand with a water/cement ratio of 0,95 by weight was used for the mortar (Class I). The average compressive strength of the mortar was 10,3 MPa at 28 days on testing a sample of 30 mortar cubes of 70 mm dimension. English bond panels with 5 mm thick mortar joints were fabricated. The dimensions of the test panel were 360 mm x 360 mm x 110 mm. The details of test panels are shown

in figure 1. To ensure uniform workmanship, all test panels were constructed by the same mason and cured under damped condition for 28 days before testing.

## Loading arrangement

The loading arrangement for testing the brick masonry panels under pseudo dynamic biaxial compression-compression loading is shown in figure 2. A biaxial state of stress was achieved by applying in-plane loads with the use of two hydraulic jacks aligned in two orthogonal directions as shown in figure 2. The two jacks were connected to a single RME control unit and thus maintaining a uniform oil pressure in the jacks during the loading history. Each of the two hydraulic jacks was of 3 000 kN capacity. A 1 000 kN capacity load cell was placed in series with each jack in the two directions of loading. A steel beam of box section stiffened using vertical stiffeners was used for load distribution. The steel beam is supported by the vertical jack at one end and by a roller at the other end. The ratio of principal stresses  $f_n/f_p$  was varied by moving the vertical jack or the roller support or both along the span of the distribution beam. To minimise the effect of platen restraint and thus ensure a more uniform state of stress in the model, 10 mm thick teflon sheets were used on all four bearing surfaces of the brick masonry specimen.

## Instrumentation

The masonry panels were instrumented with LVDTs (linearly variable displacement transducers) aligned in mutually orthogonal directions on both sides of the panel, as shown in figure 3. The LVDTs were installed to measure the axial and lateral displacement over a fixed gauge length. A gauge length of 250 mm was adopted for measurement of both axial and lateral deformations. A Pentium-based data acquisition and control software system was used to display monitor and record the load and displacement measurements in real time. The load versus axial displacement at the two locations on each side of the panel was plotted in real time during the test. The plots of axial displacement versus lateral displacement were also obtained at the same locations.

## Test procedure

Tests on the calcium silicate brick masonry specimens were conducted for the following ratios of principal stresses:

$$f = f_n/f_p = 0, 1, 2, 4 \text{ and } 10$$

Three types of tests (test types I, II and III) were conducted for each ratio

of principal stresses. A minimum of three specimens were tested for each type of test. A total of 60 specimens were tested. The three types of tests conducted are described as follows:

- *Test type I (envelope test):* Specimens were tested by increasing the load

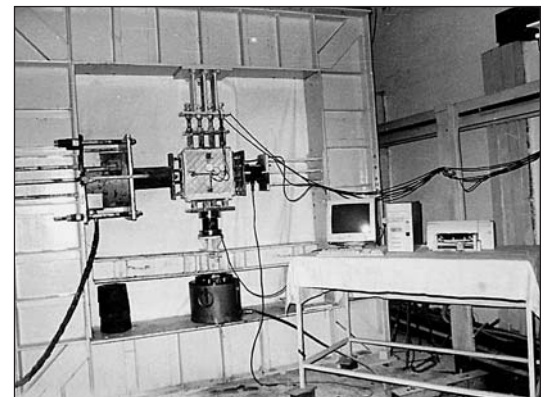


Figure 2 Pseudo dynamic biaxial compression test set-up

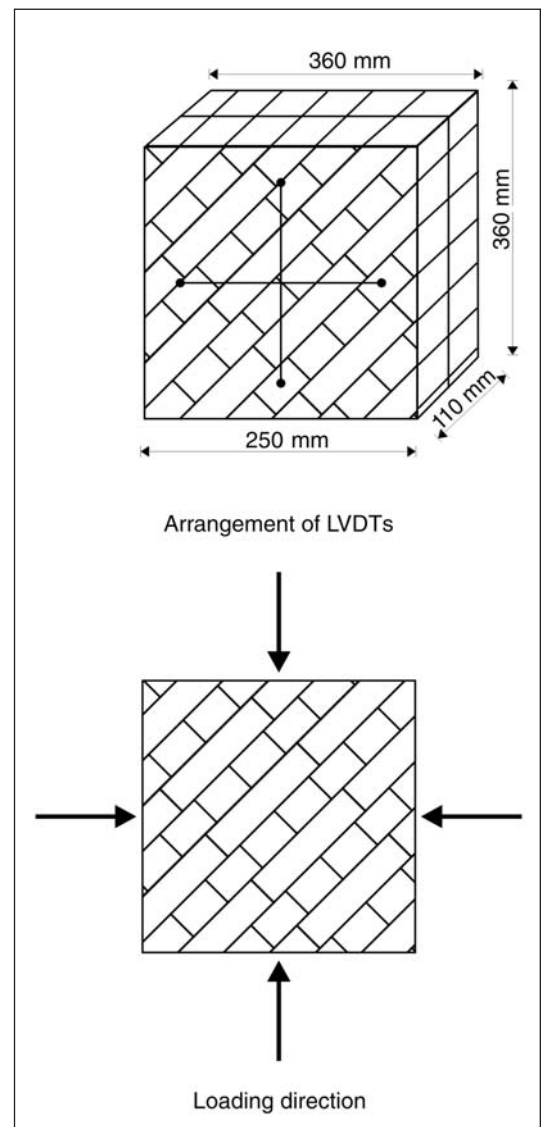


Figure 3 Arrangement of LVDTs and loading directions

steadily until failure of the specimen and a critical envelope stress-strain curve was established. For any given principal stress ratio, either the  $f_n-e_n$  curve or the  $f_p-e_p$  curve would govern the failure of the brick masonry specimen, which in turn defines the critical envelope stress strain curve wherein the parameters  $e_n$  and  $e_p$  represent the strain parallel to vertical stress and strain parallel to horizontal stress respectively.

- **Test type II (common point test):** Specimens were tested under pseudo dynamic loading in which the peak of critical principal compressive strain in each cycle of loading coincided with its envelope curve. In the ascending zone, the loading was controlled by applying an incremental increase in strain. In the descending branch of the principal compressive stress-strain curve, the load was released when an imminent descent in the loading curve was detected. The stress-strain curve obtained from the test displayed a locus of common points. A typical pseudo dynamic stress-strain curve obtained from a common point test is shown in figure 4a.
- **Test type III (stability point test):** In this test, each cycle of test type II is repeated several times until the common point stabilises at a lower bound establishing what is termed as stability point on the pseudo dynamic stress-strain history. A typical pseudo dynamic stress-strain curve obtained from a stability point test is shown in figure 4b.

In conducting the above types of test, loads were applied at an approximate rate of 3,0 MPa per minute and released at an approximate rate of 6,0 MPa per minute.

## TEST RESULTS AND EVALUATION

### Failure mode

For high stress ratios (low  $f_p$  stress), the panels with bed joint angles ( $\theta$ ) of  $0^\circ$  displayed a typical mode of failure due to splitting of bricks through vertical plane and splitting of the face joints, induced by the disparate

stress-strain characteristics of the weaker mortar and the stronger bricks. Numerous micro-cracks developed parallel to the direction of the applied load. The eventual collapse of the panels was precipitated by widening of some of these micro-cracks into major cracks. In case of the test specimens

with bed joint inclination of  $90^\circ$  to the horizontal, the load acted parallel to the bed joints resulting in a failure due to splitting of the panel along the vertical face joints. The splitting initiates at free edges and gradually propagates towards the centre of the panel. Thereafter, the separated fragments of

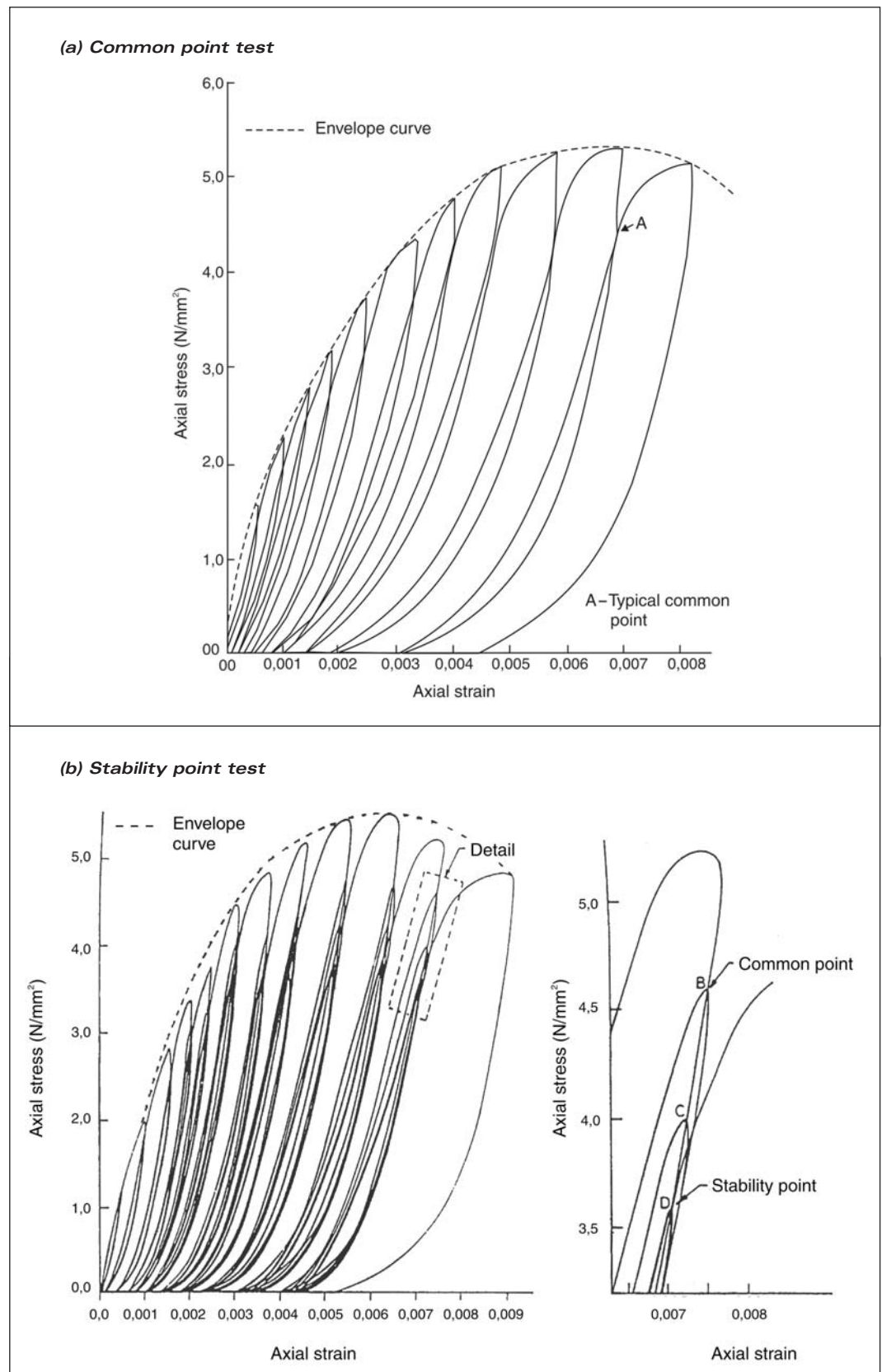


Figure 4 Typical stress-strain hysteresis curves under pseudo dynamic biaxial compression

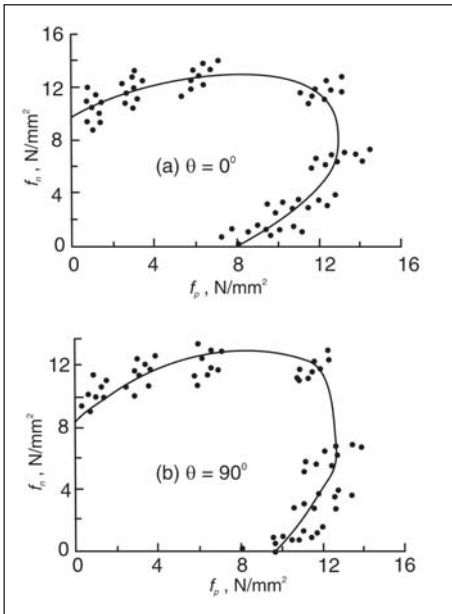


Figure 5 Failure interaction curves

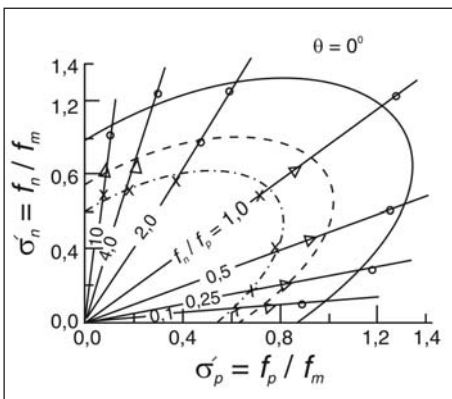


Figure 6 Family of interaction curves of peak stresses on envelope, common point and stability point curves

the panel behave like individual compression members. For low stress ratios, the splitting failure mode was limited by the second principal compressive stress for most stress ratios. Failure typically occurred in an abrupt manner due to splitting in a plane parallel to the free surface of the specimen at mid thickness irrespective of the bed joint angles. The spalling failure occurred suddenly in a brittle manner and often begins at one of the loaded edges and propagated into the panel.

### Failure interaction curve

The principal stresses at failure obtained from the experimental study are plotted in figure 5. In case of  $\theta = 0^\circ$ , the points on failure surface corresponding to the stress ratios of 0,5, 0,25, 0,10 and 0 were obtained from the failure surface corresponding to  $\theta = 90^\circ$ . A general form given in equation 1 was found suitable in defining the failure interaction curve for calcium silicate brick masonry under pseudo dynamic biaxial compression-compression loading.

$$CJ_2 + (1-C)I_1 + CI_2 = 1 \quad (1)$$

Where,  $J_2$ ,  $I_1$  and  $I_2$  are principal stress invariants defined as:

$$J_2 = \left( \frac{f_n}{f_m} - \frac{f_p}{f_m} \right)^2 \quad (2a)$$

$$I_1 = \left( \frac{f_n}{f_m} + \frac{f_p}{f_m} \right) \quad (2b)$$

$$I_2 = \left( \frac{f_n \cdot f_p}{f_m \cdot f_m} \right) \quad (2c)$$

The value  $f_m$  is the average uniaxial compressive strength normal to the bed joint.  $C$  is a constant in equation 1, which governs the nature of the failure interaction curve. For  $C = 1$ , equation 1 reduces to the Von Mises yield criterion. Values of  $C$  equal to 1,6 for the bed joint inclinations equal to  $0^\circ$ , and  $90^\circ$  to the horizontal, result in failure surfaces that provide a reasonable fit with the experimental data. The theoretically evaluated failure interaction curve together with the experimental values of  $f_n$  and  $f_p$  at failure are shown on the  $f_n$ - $f_p$  coordinate plane in figure 6.

### Family of interaction curves

The pseudo dynamic test II displayed a locus of common points and pseudo dynamic type III displayed a locus of common points and stability points. The averaged peak stresses of envelope point, common point and stability point are used to plot family of failure interaction curves. The family of failure interaction curves are plotted in a non-dimensional form as shown in figure 6. These curves have been normalized with respect to uniaxial compressive strength for load normal to the bed joint ( $\theta = 0^\circ$ ). The stress parameter  $\sigma_n$  and  $\sigma_p$  represent the non-dimensional stress parameters. Value of  $\sigma_n$  and  $\sigma_p$  are obtained by normalising the vertically applied stress,  $f_n$ , with respect to the failure (peak) stress,  $f_m$ , of each specimen.

The equation (1) of failure envelope interaction curve for brick masonry in biaxial compression could be used to model the common and stability point interaction curves at each principal stress ratio by introducing a factor  $\gamma$  in equation 1 as follows:

$$X_1 \left( \frac{\sigma'_n}{\gamma} - \frac{\sigma'_p}{\gamma} \right)^2 + (1-X_1) \left( \frac{\sigma'_n}{\gamma} + \frac{\sigma'_p}{\gamma} \right) + X_1 \frac{\sigma'_n \sigma'_p}{\gamma^2} = 1,0 \quad (3)$$

Where

$$X_1 = 1 + f_p/f_n \quad (4a)$$

$$\sigma'_n = f_n/f_m \quad (4b)$$

$$\sigma'_p = f_p/f_m \quad (4c)$$

The values  $f_m$  is the average uniaxial compressive strength normal to the bed joint ( $\theta = 0^\circ$ ). The variation of the factor  $\gamma$  in equation 3 accounts for the change in the

stress at the maxima of the envelope, common point and stability point curves for a given principal stress ratio. The peak stress of common point and stability point curves for any principal stress ratios can be obtained by assessing suitable values for  $C$  and  $\gamma$  in equation 3. The value of  $C$  is 1 and  $\gamma$  for envelope, common point and stability point interaction curves are 1,0, 0,74 and 0,62 respectively.

In general, the computed interaction curves and the experimental value of the failure stress from the test results showed reasonable agreement. Thus the interaction curves presented in Figure 6 provide a method of computing absolute stress at the peak of the envelope curve, common point curve and stability point curve for any principal stress ratio for the given uniaxial strengths of calcium silicate brick masonry in compression-compression stress state region. The analytical envelope, common point and stability point interaction curves for  $0^\circ$  is shown in figure 6. The orthogonal rotation of figure 6 for  $0^\circ$  gives interaction curves for  $90^\circ$ .

### Significance of stability point curve

The point of intersection of loading and unloading curves is known as the common point. The stresses above the common point produce additional strain, while stresses below these points will result in the stress-strain path going into a loop where the point of intersection of the reloading curve and unloading curve descends and stabilises at a lower bound called the stability point. If a locus of stability points can be identified on the pseudo dynamic stress-strain history of brick masonry, then this can be a valuable contribution for the design of some brickwork structures where reductions of compressive strength due to the effect of alternating live loads have to be taken into account.

### CONCLUSIONS

Failure interaction curves have been derived in terms of principal stress and bed joint orientation. The mode of failure of panels was found to be significantly influenced by the ratio of the horizontal to the vertical load and the bed joint orientation. Most panels were found to split along a plane parallel to the free surface at lower stress level. An equation for the failure interaction curve was proposed in terms of stress invariants and the principal stress ratio at any general stage of loading. The proposed failure curve showed a reasonably good fit with the experimental results. For lower stress ratios, the bed joint orientation did not play a significant role. However, when one principal stress predominates, joint properties will play a significant role. The envelope curve under pseudo dynamic loading coincided with the stress-strain curves under monotonic loading. A locus of common points and a locus of stability points were obtained from the pseudo dynamic stress-strain curves. A general analytical expression was

proposed for the envelope interaction curves, common point interaction curves and stability point interaction curves. By assigning suitable values for equation parameters, the expression can be used to determine the peak stress of envelope curve, common point curve, or the stability point curve. Reasonable fit was obtained with the experimental data. The stability point interaction curve provides a rational design tool in defining the permissible stress level for calcium silicate brick masonry under in-plane pseudo dynamic loading.

### References

- Allen, H 1973. Effect of direction of loading on compressive strength of brick masonry. *Proceedings of the Third International Brick Masonry Conference, Essen*, pp 98–105.
- Alshebani, M M 1999. Response of brick masonry under cyclic loading. Thesis presented to the Indian Institute of Technology, Delhi, India, in partial fulfilment of the requirements for the degree of Doctor of Philosophy.
- Dhanasekar, M 1985. The performance of brick masonry subjected to in-plane loading. PhD thesis, University of Newcastle, Australia.
- Dhanasekar, M, Kleeman, P W & Page, A W 1985. Biaxial stress-strain relations for brick masonry. *Journal of Structural Engineering, ASCE*, 3(5):1085–1100.
- Khalaf, F M 1997. Brickwork masonry compressed in two orthogonal directions. *Journal of Structural Engineering, ASCE*, 123(5):591–596.
- Naraine, K & Sinha, S N 1992. Stress-strain curves for brick masonry in biaxial compression. *Journal of Structural Engineering, ASCE*, 118(6):1451–1461.
- Page, A W 1981. The biaxial compressive strength of brick masonry. *Proceedings of the Institution of Civil Engineers*, 2(71):893–906.
- Page, A W 1982. An experimental investigation of the biaxial strength of brick masonry. *Proceedings of the Sixth International Brick Masonry Conference, Rome*, pp 3–15.
- Samarasinghe, W & Hendry, A W 1980. Strength of brickwork under biaxial stresses. 7th International Symposium on Load Bearing Brickwork, British Ceramic Society, London.
- Samarasinghe W 1980. The in-plane failure of brickwork. PhD thesis, University of Edinburgh.